



**HAL**  
open science

## The origins of thixotropy of fresh cement pastes

Nicolas Roussel, Guillaume Ovarlez, Sandrine Garrault, Coralie Brumaud

► **To cite this version:**

Nicolas Roussel, Guillaume Ovarlez, Sandrine Garrault, Coralie Brumaud. The origins of thixotropy of fresh cement pastes. *Cement and Concrete Research*, 2012, 42, pp.148-157. 10.1016/j.cemconres.2011.09.004 . hal-00705595

**HAL Id: hal-00705595**

**<https://hal.science/hal-00705595v1>**

Submitted on 12 Dec 2024

**HAL** is a multi-disciplinary open access archive for the deposit and dissemination of scientific research documents, whether they are published or not. The documents may come from teaching and research institutions in France or abroad, or from public or private research centers.

L'archive ouverte pluridisciplinaire **HAL**, est destinée au dépôt et à la diffusion de documents scientifiques de niveau recherche, publiés ou non, émanant des établissements d'enseignement et de recherche français ou étrangers, des laboratoires publics ou privés.

# 1 THE ORIGINS OF THIXOTROPY OF FRESH CEMENT PASTES

2

3 N. Roussel<sup>1\*</sup>, G. Ovarlez<sup>2</sup>, S. Garrault<sup>3</sup>, C. Brumaud<sup>1</sup>.

4

5 <sup>1</sup> Université Paris Est, IFSTTAR, France.6 <sup>2</sup> Université Paris Est, Laboratoire Navier (UMR CNRS), France.7 <sup>3</sup> ICB, UMR/CNRS 5209, France.

8

9 \* : Corresponding author, tel.: +33140435285, [nicolas.roussel@lpc.fr](mailto:nicolas.roussel@lpc.fr)

10

## 11 ABSTRACT

12 In this paper, we study the thixotropic behavior of standard fresh cement pastes, and show  
13 that it may find two origins. We first clarify the ambiguity in literature concerning the critical  
14 strain of fresh cement pastes, thanks to a detailed analysis of their macroscopic behavior. We  
15 show that the largest critical strain can be associated to the network of colloidal interactions  
16 between cement particles whereas the smallest critical strain can be associated to the early  
17 hydrates, which form preferentially at the contact points between aggregated cement grains.  
18 From the study of the structuration kinetics of the macroscopic properties (elastic modulus,  
19 yield stress) associated with these two strain scales, we show that there exists a short term  
20 thixotropy due to colloidal flocculation with a characteristic time of the order of a few  
21 seconds along with a long term thixotropy (of practical interest) due to the ongoing hydrates  
22 nucleation. From a simple dimensional approach, we moreover suggest why the apparent  
23 yield stress of the mixture left at rest can be approximated as a linear function of time.

24

## 25 1. Introduction

1

2 The vast majority of cementitious materials are able to support a finite amount of stress  
3 without flowing. Macroscopic flow is however achieved as soon as the stress applied to the  
4 system overcomes what can be supported by the network of particles in interaction. This  
5 critical value is called yield stress and is the dominant intrinsic parameter of what is called in  
6 practice workability of concrete [1, 2].

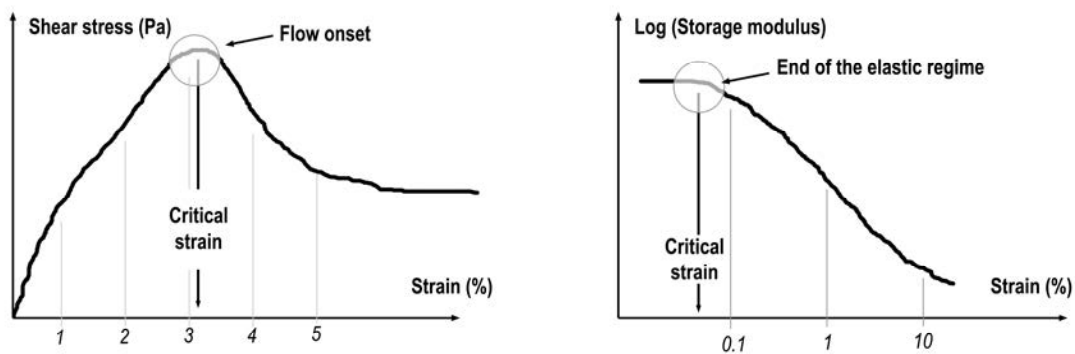
7 In many cementitious materials, a reversible evolution of the material rheological behavior is  
8 often noted during the so-called dormant period of the hydration reaction: at rest, the apparent  
9 yield stress (or static yield stress) continuously increases [1-9]. As this evolution can be  
10 erased by a strong shearing or remixing of the paste and the material can be brought back to a  
11 reference state, it is often described as thixotropy. The origin of this evolution is however  
12 very unclear. The word “structuration” is therefore often used to describe the consequences of  
13 this thixotropic behavior as this word is not associated to a specific physical phenomenon [8,  
14 9]. It only implies that a structure is being built or destroyed within the material all along its  
15 flow history. As this structural evolution is macroscopically reversible, most explanations  
16 available in literature focus on microscopic reversible physical phenomena, such as reversible  
17 colloidal flocculation and deflocculation. Very various phenomena can however be at the  
18 origin of thixotropy for other materials in nature or industry. Of course, reversible colloidal  
19 flocculation may explain thixotropy in many suspensions but reversible entanglement of  
20 polymer chains or reversible orientation of Brownian slender particles are also potential  
21 explanations for macroscopic thixotropic behavior [3].

22 Yield stress is dictated by the structure and strength of the network of cement particles in  
23 interaction [10, 11]. Accumulated experimental and numerical evidence show that network  
24 rupture in particles suspension occurs when its initial structure has been sufficiently modified,  
25 namely for a critical strain  $\gamma_c$  [12-14]. This critical strain and the yield stress should then be

1 related by  $\tau_0 = G\gamma_c$  where  $G$  is the shear elastic modulus as long as we assume a linear  
 2 elastic behavior in the solid regime below the yield stress.

3 There is however a strong ambiguity in the literature concerning the value of the critical strain  
 4 of cement pastes. When Mahaut *et al.* [15] or Schmidt and Schlegel [16] study the transition  
 5 from rest to flow (Fig. 1), they measure a critical strain of the order of several % while other  
 6 studies using oscillary rheometry (Fig. 1) point towards values of the order of few hundredths  
 7 of % [17, 18]. A better understanding of the mechanisms of yielding, which is crucial for the  
 8 understanding of the origin of thixotropy, implies that this ambiguity has to be understood.

9



10

11 *Figure 1. The two critical strains in literature (sketch). (left) : critical strain of the order of a few % in*  
 12 *a yield stress measurement; (right) : critical strain of the order of a few hundredths of % in a storage*  
 13 *(or elastic) shear modulus measurement.*

14

15 Let us first note that, in the above four papers, what is called “flow onset” or “critical strain”  
 16 strongly differs. In the first case [15, 16], flow onset is associated to strong structural changes  
 17 in the material. During this type of experiments, a shear stress is measured as a function of  
 18 time while applying a low constant strain rate. The rheological tools can be parallel plates,  
 19 coaxial cylinders or Vane test. Only the peak in the shear stress curve in Fig. 1 (left) is  
 20 considered as it is when the applied stress is higher than this peak value that the material

1 flows in terms of practical applications. This value is called apparent or static yield stress [9,  
2 19]. For example, in the case of shotcrete, it is this critical value that will control if the  
3 material stays on the wall in thick layers rather than flow down. When this type of  
4 measurement is carried out on concrete, mortar or cement paste after a resting time no longer  
5 than a few minutes, the critical strain associated to the peak value is usually of the order of a  
6 few %.

7 In the second case [17, 18], the measured critical strain is associated to the end of the linear  
8 elastic regime. Strain oscillations of increasing amplitudes are applied to the tested material.  
9 The frequency of the oscillation is of the order of 1Hz and the elastic shear modulus of the  
10 material is computed from the measured stress [17, 18]. The critical strain is defined by the  
11 onset of an important decrease of shear modulus as shown in Fig. 1(right) and not, as above,  
12 by a true measurement of the flow onset. As flow in simpler materials, like model colloidal  
13 suspensions [20], corresponds to the end of the elastic regime, this is a natural way to measure  
14 a critical strain. For many materials in nature or industry, both definitions and measurement  
15 protocols then lead to a more or less identical value of the critical strain [20-22]. The  
16 discrepancies between both values in the case of cement pastes would then mean that, at the  
17 smallest critical strain, the system does not really begin to flow and does not experience any  
18 reorganization of the cement particle network.

19 The aim of the first part of this paper is to understand the difference between the two critical  
20 strains described above, and to show how the mechanisms at the origin of this difference  
21 affect yield stress and thixotropy. We first show that, in fact, there does not exist only one but  
22 at least two critical strains in fresh cement pastes. Our observations suggest that the largest  
23 critical strain can be associated to the breakage of the network of colloidal interactions  
24 between cement particles, which forms shortly after the end of mixing, and that the smallest

1 critical strain can be associated to the breakage of the early hydrates, which form  
2 preferentially at the contact points between flocculated cement grains.

3 In the second part of this paper, from the study of the structuration kinetics of the  
4 macroscopic properties (elastic modulus, yield stress) associated with these two strain scales,  
5 we suggest that there exists a short term thixotropy due to colloidal flocculation with a  
6 characteristic time of the order of a few seconds along with a long term thixotropy (of  
7 practical interest) due to the ongoing hydrates nucleation. From a simple dimensional  
8 micromechanical approach, we moreover explain why apparent or static yield stress of the  
9 mixture left at rest can be approximated, in most cases, as a linear function of time.

10

## 11 **2. Origin of the two critical strains of fresh cement pastes**

12 In order to clarify the ambiguity about the critical strain in literature, we first study the  
13 macroscopic behavior of a pure cement paste (*i.e.* no organic or mineral admixtures) during  
14 both yield stress measurement and elasticity measurement. We focus on both small and large  
15 strains and compare the information that can be obtained from both techniques.

16

### 17 **2.1. Experimental measurements**

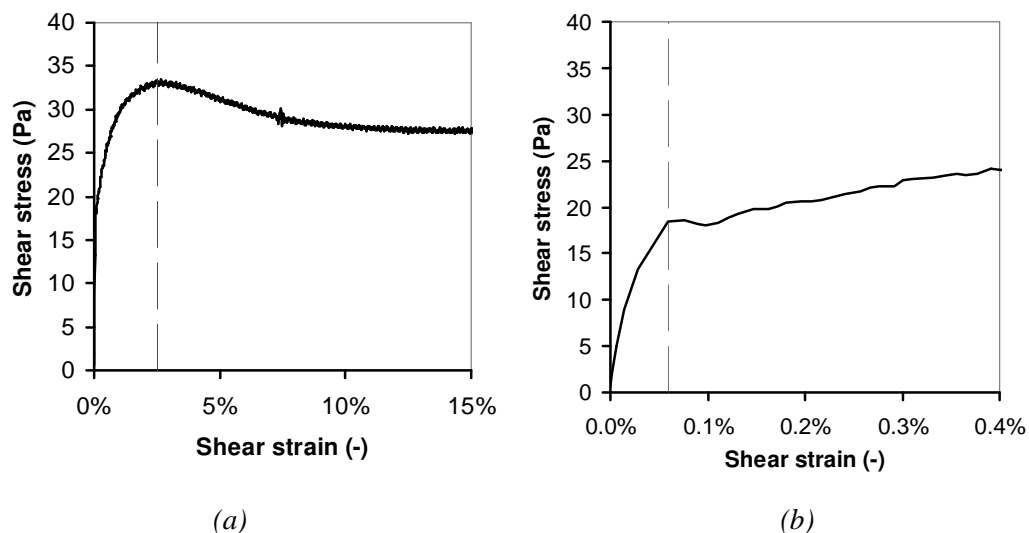
18

19 We plot in Fig. 2 the results of a Vane test experiment on a cement paste (water to cement  
20 weight ratio  $W/C = 0.4$ ). The cement is a CEM I from Lafarge, Le Havre, France. The  
21 measurements are carried out using a *C-VOR Bohlin*<sup>®</sup> rheometer. The Vane geometry is a  
22 four-bladed paddle with a diameter of 25 mm, the outer cup diameter is 50mm and its depth is  
23 60 mm. 20 minutes after the end of the mixing phase, the cup of the rheometer is filled and  
24 the sample is sheared at  $150 \text{ s}^{-1}$  during 200 s. After a 5 minutes resting time, a constant shear  
25 rate of  $0.005 \text{ s}^{-1}$  is applied to the sample. After an initial increase of the shear stress, the stress

1 peak is followed by a plateau representative of steady state flow. The main feature in Fig. 2(a)  
 2 is the flow start for a critical shear strain equal to 2.5 %. The associated static or apparent  
 3 yield stress (*i.e.* the stress peak) is of the order of 32 Pa whereas the stress at the plateau is of  
 4 the order of 27 Pa.

5 If we now zoom on the first few tenths of % strain in Fig. 2(b), we can however spot another  
 6 feature, far less visible than the first one when using standard linear scales. In the very first  
 7 stages of the shearing process, the shear stress first increases very rapidly with the shear  
 8 strain: this would correspond to the behavior of a very stiff material. Then, for a critical shear  
 9 strain of the order of 0.05 %, there is an abrupt change of the stress/strain slope: the shear  
 10 stress starts increasing very smoothly with the shear strain, which corresponds to what is  
 11 usually observed as in Fig. 2(a). It can then be noted that the instantaneous (or apparent) shear  
 12 modulus (*i.e.* the ratio between shear stress and shear strain) for strains lower than a few  
 13 hundredths of % is of the order of several thousands of Pa whereas it is of the order of several  
 14 hundreds of Pa at the stress peak.

15



16

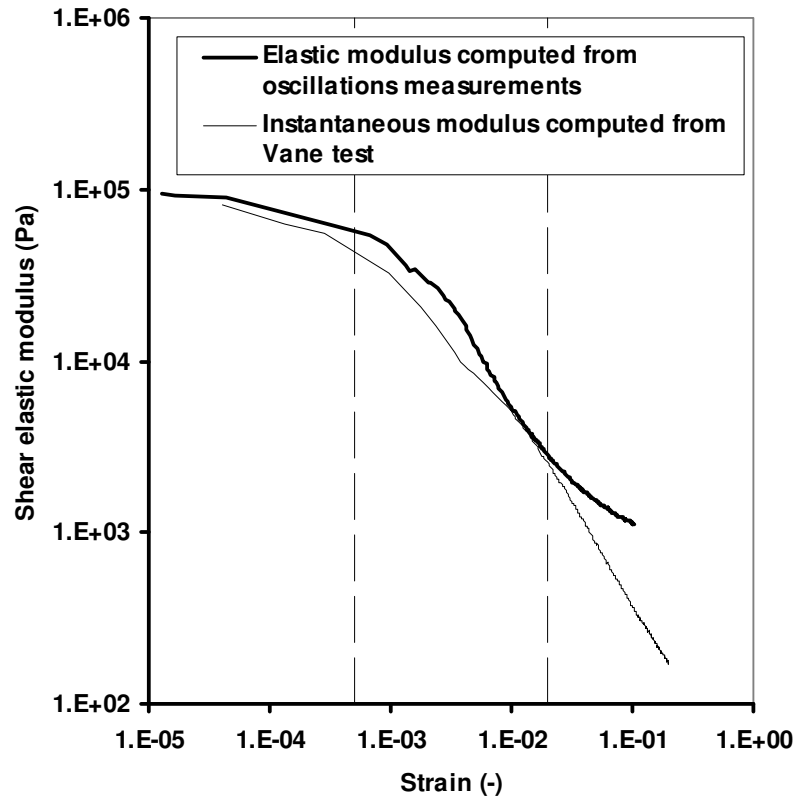
17

18 *Figure 2. Shear stress as a function of shear strain during a Vane test on a cement paste with a water*  
 19 *to cement ratio of 0.4. (a) Linear shear strain scale from 0 to 15%; (b) Linear shear strain scale from*  
 20 *0 to 0.4%.*

21

1 The shear storage modulus  $G'$  is usually measured in oscillation experiments. The classical  
2 experiment then consists in applying strain oscillations and in measuring the stress response.  
3 As elastic effects are in phase with the strain whereas viscous effects are in phase with the  
4 strain rate (and thus in quadrature with the strain), this defines an elastic modulus  $G'$  and a  
5 viscous modulus  $G''$ . It is also possible to define a complex modulus  $G^* = G' + iG''$ . When  
6 viscous effects can be neglected (*i.e.* low shear rates or solid behavior),  $G'$  should be of the  
7 same order of magnitude as the instantaneous (or apparent) shear modulus, which is defined  
8 as the instantaneous ratio between shear stress and shear strain during a yield stress  
9 measurement such as the one in Fig. 2. We compare in Fig. 3 these two *moduli* in the case of  
10 the same cement paste as in the above section. The instantaneous shear modulus is calculated  
11 from the above Vane test result at  $0.005 \text{ s}^{-1}$  by dividing the measured shear stress by the shear  
12 strain whereas the shear storage modulus  $G'$  is measured at an oscillation frequency of 1Hz  
13 as a function of the strain amplitude between  $1.10^{-5}$  to  $1.10^{-2}$ . In both cases, the Vane tool  
14 described above is used. 20 minutes after the end of mixing, the material is pre-sheared at  $150$   
15  $\text{s}^{-1}$  for 200 s before the measurement. The test starts after a five minutes resting time.  
16 We see in Fig. 3 that, below a few hundredths of % of strain, both storage and instantaneous  
17 shear *moduli* are roughly constant defining an elastic linear regime. The brutal drop in  
18 instantaneous shear modulus in Fig.2(b) can therefore be associated to the critical strain  
19 defined as the end of the linear elastic regime in [17]. We also see that, below a few % both  
20 *moduli* have the same order of magnitude while, from Fig.2(a), we know that flow has not  
21 started yet in the material: this means that, in contrast with simple yield stress fluids [20-22],  
22 the strong decrease in the elastic modulus of cement pastes with strain cannot be interpreted  
23 directly as a signature of yielding.





1  
 2 *Figure 3. Shear elastic modulus as a function of strain. The oscillation frequency is 1Hz and the strain amplitude*  
 3 *is increased from  $1.10^{-5}$  to  $1.10^{-1}$ . The shear rate is  $0.005s^{-1}$  for the Vane test. The two dashed vertical lines*  
 4 *correspond to the two critical shear strains.*

5  
 6 To summarize, we see that looking at both standard yield stress measurement and elastic  
 7 modulus measurement provides a macroscopic description of two critical strains of cement  
 8 pastes, which both exist simultaneously. The first critical strain is clearly associated with a  
 9 very stiff elastic behavior of the material at low strain, while the second critical strain is  
 10 associated with yielding and flow onset. The following section is devoted to the discussion of  
 11 the microscopic origin of these critical strains. It may be useful to keep in mind at this stage  
 12 that a critical strain as defined here is associated to an important change in the mechanical  
 13 properties. Although the stress needed to reach this critical strain may result from the  
 14 contribution of various phenomena, the value of the critical strain provides a strong signature  
 15 of the dominant phenomenon. E.g., rigid and fragile materials have low fracture critical

1 strains whereas organic polymer based materials, for instance, often display critical strains  
2 which are order of magnitudes larger.

3

## 4 **2.2. The smallest critical strain : the CSH contribution**

5

6 To understand the origin of the first critical strain, let us first comment its value. A critical  
7 macroscopic strain  $\gamma_c$  of order of a few  $10^{-4}$  means that, at a local scale, the relative  
8 movement  $\delta$  of two neighboring cement particles is reversible as long as it is inferior to  
9  $\gamma_c d \approx$  a few nm where  $d \approx 10 \mu\text{m}$  is the typical size of a cement particle. This would mean  
10 that there are some links of size of the order of a few nm between the cement particles that are  
11 broken for strains higher than the first critical macroscopic strain.

12 Confirmation of this first basic interpretation and a better insight on the nature of these links  
13 is gained from existing literature. The storage shear modulus measured below the lowest  
14 critical strain during the dormant period is actually usually seen to continuously increase in  
15 time [17, 23]. This continuous increase has previously been associated to the formation of  
16 hydrates by Lei and Struble [23] in the case of cement pastes and Nachbaur *et al.* [17] in the  
17 case of both tri-calcium silicate and cement pastes. These authors suggested that the  
18 evolutions of the system before setting are the signatures of the CSH nucleation during the  
19 dormant period. These CSH were described as forming “bridges” between cement particles.  
20 After what was described in the above papers as the first short term coagulation phase, a long  
21 term second phase in the evolution of the elastic shear modulus was called rigidification in  
22 [24, 25].

23 Several important experimental facts from the above papers confirm these interpretations:

24 A) As we pointed out above, the breakage of an inter-particle bond such as CSH particles  
25 that has a range  $\delta$  of a couple nm with respect to cement particles whose size  $d$  is of

1 the order of 10 microns would give a macroscopic critical strain  $\delta d$  in the range of a  
2 few hundredths of %.

3 B) Pseudo contact zones between grains are preferential sites for nucleation. This can  
4 explain that, although the degree of hydration is close to zero, the consequences of the  
5 CSH nucleation are strong at a macroscopic level as they nucleate specifically in very  
6 crucial zones in the interacting particles network.

7 C) This critical strain is of the same order of magnitude as the critical strain for which  
8 cracks propagate in hardened concrete. It is also, in the case of hardened concrete, the  
9 end of the elastic linear regime.

10 It has to be kept in mind that, in cement pastes, other early hydration products than CSH  
11 could nucleate and have macroscopic consequences on the rheological behavior. We will  
12 however in this paper follow the above authors and keep on assuming that the nucleating  
13 products at the origin of the rigidification process are CSH for the following reasons:

14 A)  $C_3S$  pastes in [17] had a similar rigidification behavior as standard cement pastes and  
15 CSH nucleation was sufficient to explain the measured behavior without any  
16 contribution from any other hydration products.

17 B) Most other potential hydration products are far bigger than a few nm and can not  
18 therefore nucleate in the pseudo-contact zones between flocculated cement particles in  
19 which the separating distance between cement grains surfaces is of the order of a few  
20 nm [26]. Nucleation at any other locations in the system, as long as the volume  
21 fraction of the nucleated products remains low, shall not have any major consequences  
22 on the rheological behavior of the system.

23 C) All measurements in this paper are carried out at least 20 minutes after mixing. The  
24 early hydration reactions have already occurred in the system. Their consequences in  
25 terms of cement particles interactions are erased by the strong pre-shearing described

1           above before each test. Because of this specific procedure, no structural breakdown  
2           may be spotted [1].

3   Finally, this leads to interpreting the first critical strain as a signature of the breaking of CSH  
4   links between cement particles. In order to simplify our text in the following, we will from  
5   now on call the smallest critical strain, below which very high values of the storage modulus  
6   are measured, the **rigid critical strain** in opposition to the soft **colloidal critical strain**  
7   described below. It will however be necessary to keep in mind that, at the nano-scale, CSH  
8   bridges can also be seen as dense suspensions of particles, the cohesion of which originates  
9   from colloidal forces (*i.e.* ion correlation forces) [27, 28]

10

### 11           **2.3. The largest critical strain : the colloidal contribution**

12   While a low critical strain had to be associated with short range links between the particles, a  
13   large critical strain certainly involves non-contact interactions between the particles: it implies  
14   rather large movement of two neighboring cement particles. This is consistent with the critical  
15   strain above which the particle start to rearrange and flow starts in many other colloidal  
16   suspensions in nature or industry [12, 13, 20] where only such interactions are involved.

17   Several types of non-contact interactions occur within a cementitious suspension [10]. At  
18   short distance, cement particles interact via (generally attractive) van der Waals forces [26].

19   Also, there are electrostatic forces that result from the presence of adsorbed ions at the surface  
20   of the particles [29]. Polymer additives (such as High Range Water Reducing Admixtures  
21   HRWRA), present in many modern cementitious materials, can induce steric hindrance [30-  
22   32], which is believed to predominate over electrostatic repulsion. Each of these different  
23   interactions introduces non-contact forces between particles, the magnitude of which depend  
24   primarily on their separation distance. Repulsive electrostatic forces alone are generally  
25   insufficient to prevent agglomeration due to van der Waals attractive forces and steric

1 hindrance or additional electrostatic repulsion from polymers is needed to disperse cement  
2 particles.

3 Due to the high particle volume fraction of cement pastes, there exists in the material a  
4 percolated network of particle-particle colloidal attractive interactions which allows the  
5 suspension to support finite amount of stress without flowing. This network breakage occurs  
6 when its initial shape has been sufficiently modified, namely for a critical strain  $\gamma_c$  of order of  
7 a few % as observed in Fig. 2a.

8

### 9 **3. Kinetics of percolation(s) and rigidification**

10

11 In the previous section, we have shown that two critical strains, which can be related to CSH  
12 and colloidal links between cement particles, exist in a given cement paste. In order to get a  
13 better insight in the macroscopic structuration of cement pastes and of its origin, we now use  
14 elastic modulus measurements with oscillation to characterize the structuration kinetics  
15 associated with both kinds of interactions between cement particles.

16

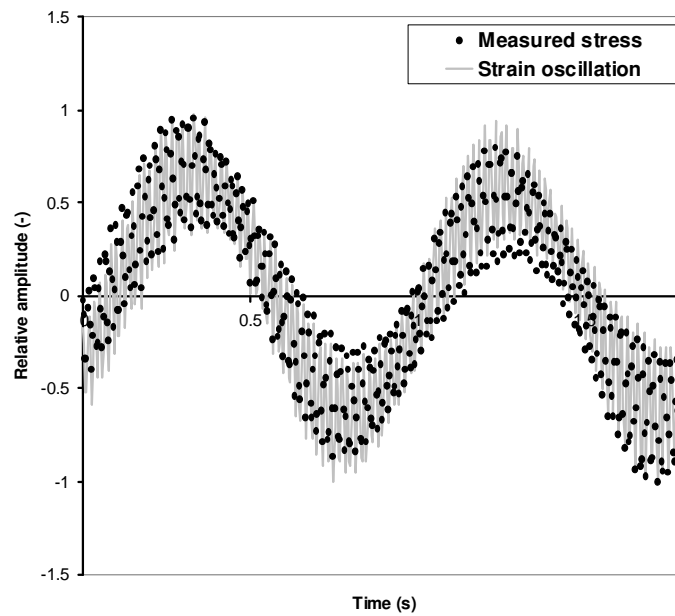
#### 17 **3.1. Macroscopic observations**

##### 18 **3.1.1. Independent macroscopic measurements of the two structuration kinetics**

19 In order to study independently the formation of the two networks, we apply oscillating  
20 strains of different amplitudes and frequencies.

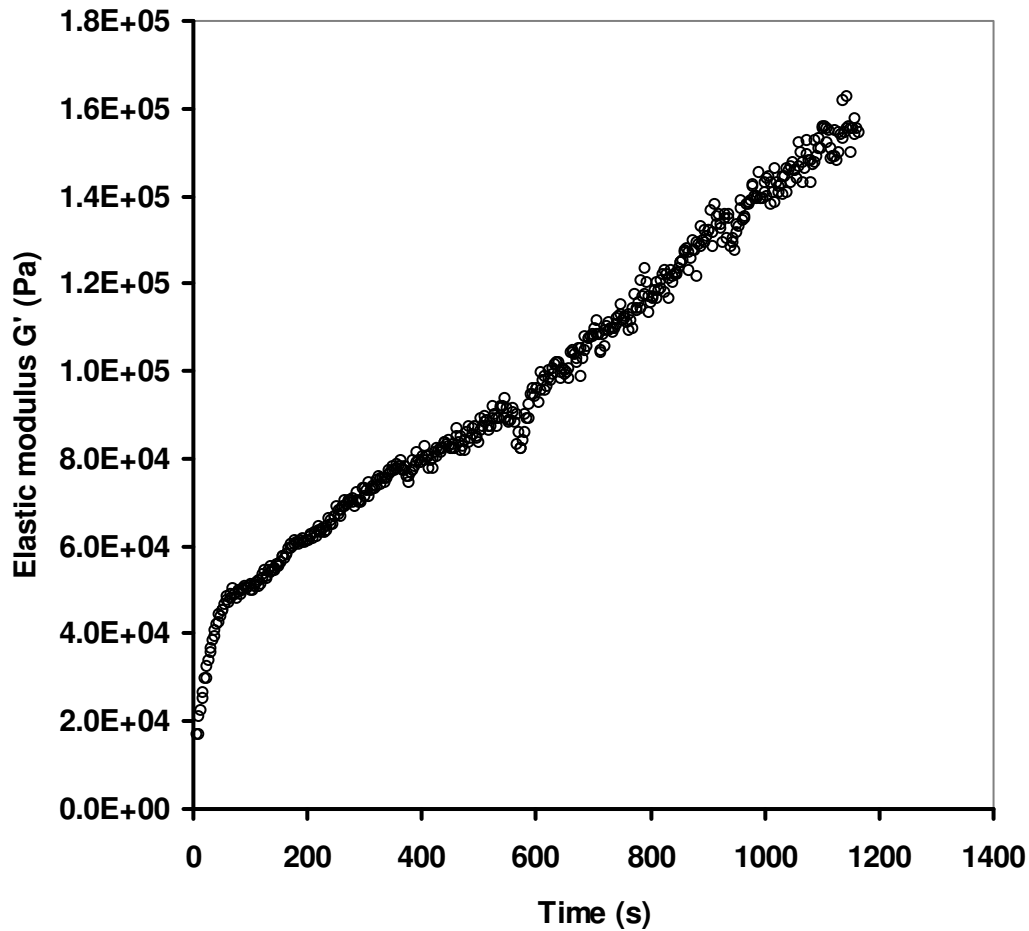
21 First, in order to measure the kinetics of the rigid interactions network evolution, we simply  
22 apply oscillations of amplitude lower than the rigid critical strain as in [17, 18]. As, below the  
23 rigid critical strain, the answer of the system is purely elastic, the measured stress is in phase

1 with applied oscillating strain as shown in Fig. 4 and the storage elastic modulus is equal to  
2 the instantaneous shear elastic modulus of the system.



3

4 *Figure 4. Relative amplitudes of applied strain and measured stress as a function of time. The*  
5 *amplitude of the strain oscillation is 0.05% and the frequency is 1Hz.*



1

2 *Figure 5. Evolution of the elastic modulus of the rigid network as a function of time. Strain*  
3 *amplitude 0.0003, frequency 1Hz.*

4

5 We measured this evolution of this modulus in the case of our cement paste. 20 minutes after  
6 mixing, we pre-sheared the paste at  $150\text{s}^{-1}$  for 150s. Straight after pre-shear, we applied an  
7 oscillating strain of amplitude 0.0003 at a 1Hz frequency. After a few hundreds seconds, the  
8 evolution of the elastic modulus becomes linear with time as shown in Fig. 5, as already  
9 measured in [17].

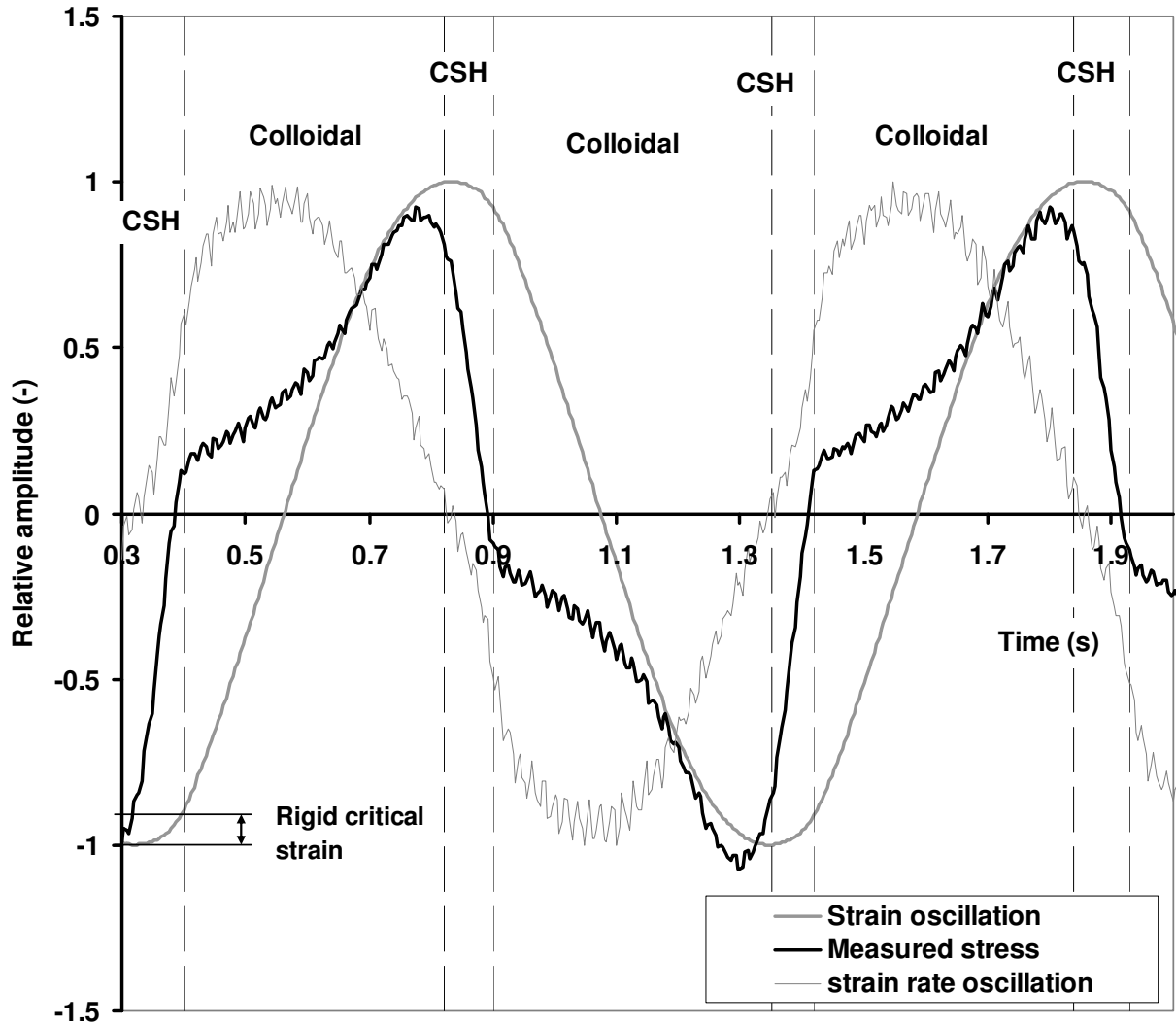
10 In order to study the kinetics of formation of the colloidal network, we should apply  
11 oscillations of amplitude larger than the rigid critical deformation (*i.e.* 0.5%). Such a

1 deformation is indeed large enough to break the CSH bridges formed between cement  
2 particles. This is however not sufficient as discussed below.

3 In Fig. 6, the relative amplitude of applied oscillating strain (*i.e.* the ratio between the applied  
4 strain and the strain amplitude) and the relative amplitude of measured stress (*i.e.* the ratio  
5 between the measured stress and the stress amplitude) are plotted as a function of time during  
6 a couple of oscillation periods at 1Hz for an amplitude of 0.005. The cement paste, the  
7 measurement protocol and the Vane tool are the same as the ones described previously in this  
8 paper. There is no resting time before test starts.

9





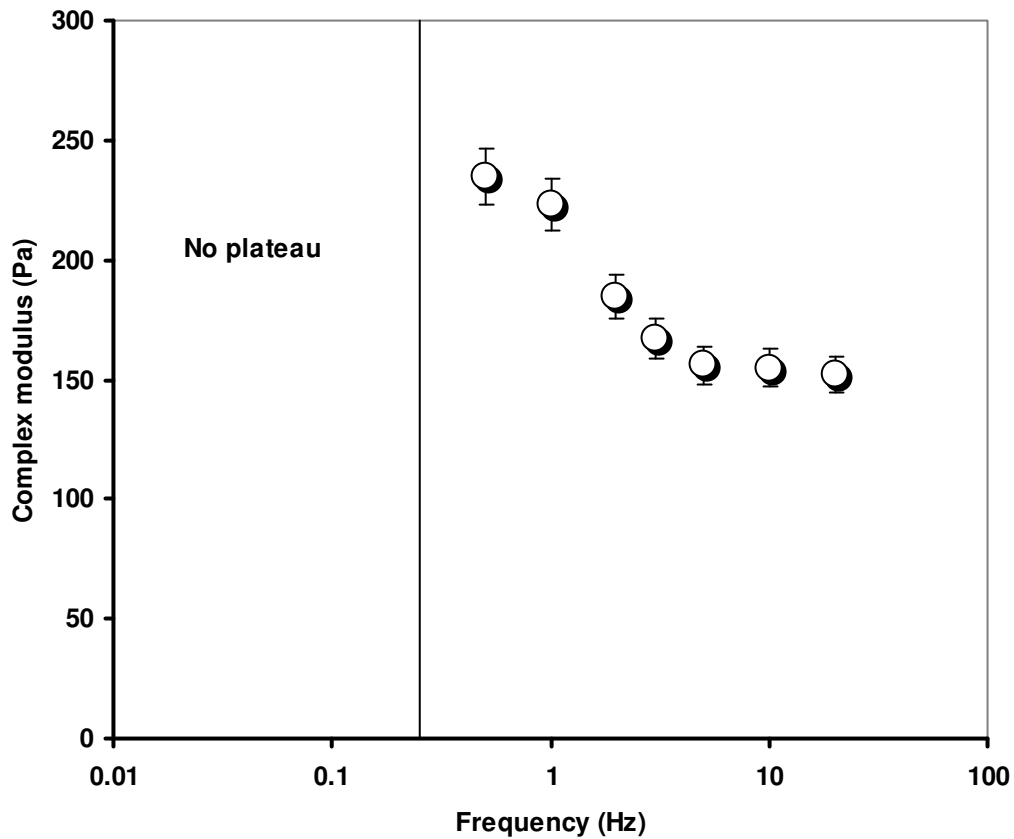
1  
 2 Figure 6. Relative amplitudes of applied strain and measured stress as a function of time. The  
 3 amplitude of the strain oscillation is 0.5%.

4  
 5 Let us comment on Fig. 6. We start at the peak of the strain oscillation, when the oscillating  
 6 shear rate is equal to zero ( $t \approx 0.3s$ ). Then, during a very short time, the system is not sheared  
 7 and can be considered as the reference initial configuration of the system. In this initial  
 8 unsheread configuration, CSH nucleate between cement particles (*i.e.* in less than a couple  
 9 tenths of seconds). As a consequence, from the point of view of these CSH, the system strain  
 10 is zero and this can be considered as their elastic reference state. As the shear rate increases ( $t$   
 11 between 0.3s and 0.4s), the shear strain increases until it reaches the rigid critical strain

1 (taking the initial configuration at  $t \approx 0.3\text{s}$  as the reference configuration). Note that, during  
2 this period, the relative slope between stress and strain is very high showing how rigid the  
3 system is. At  $t \approx 0.4\text{s}$ , the strain in the system at the scale of the CSH is of the order of one  
4 tenth of the strain amplitude (namely a strain of order 0.05%) and the CSH network breaks.  
5 Suddenly, the relative slope between stress and strain strongly decreases from 0.4 to 0.6s.  
6 From 0.6s, we suggest that most CSH have been destroyed and that the measured stress is  
7 now dictated mainly by the residual soft colloidal network (and potentially by an equilibrium  
8 between nucleation of CSH and their instantaneous destruction). The answer of this residual  
9 network is elastic as shown by the period during which both stress and strain are in phase ( $t$   
10 between 0.6s and 0.75s). When  $t \approx 0.75\text{s}$ , the oscillating shear rate reaches zero. Once again, it  
11 can be considered that, during a very short time, the system is not sheared and, again, CSH  
12 nucleate between cement particles, recreating a rigid interaction network, which will also be  
13 broken by the following relative increase in strain. It can be seen in Fig. 6 that the answer of  
14 the system is very complex: the system can be considered as visco-elasto-plastic, it can  
15 display two very different elasticities and, whereas the reference configuration shall be for  
16 zero strain, it is, at the scale of the nucleating CSH, reached every period as soon as the shear  
17 rate becomes too small to destroy them, *i.e.* at the peaks of the strain signal. Because of this  
18 complexity, some features are therefore difficult to explain: for instance, between 0.75 and  
19 0.8s, although the strain is still increasing, the measured stress is decreasing. The value of the  
20 storage modulus measured using such oscillations is therefore very difficult to analyze and is  
21 strongly affected by the equilibrium between formation and destruction of the CSH bridges  
22 between particles.

23 In order to isolate the colloidal network, we therefore not only need to apply an oscillating  
24 strain larger than the rigid critical strain in order to destroy the CSH but we also should apply  
25 it at a frequency sufficiently high to reduce the influence of the CSH nucleation when the

1 system reaches a zero strain rate configuration. In order to identify this frequency, we plot in  
2 Fig. 7 the complex modulus as function of the frequency for strain oscillations of amplitude  
3 0.005. We use the same test as above and test starts immediately after the pre-shear phase.



4

5 *Figure 7. Measured complex modulus in steady state as a function of oscillation frequency.*

6 In a first regime (below 0.2Hz), there is no steady state. The complex modulus keeps on  
7 increasing and no equilibrium between destruction and nucleation of CSH is reached. In a  
8 second regime, between 0.2Hz and 5Hz, a steady state is reached. It however depends on the  
9 frequency showing that CSH contributes to the measured stress and therefore to the computed  
10 complex modulus. As frequency increases, the role of CSH in the system decreases as the  
11 time during which they can nucleate shortens. In the last regime (above 5Hz), the complex  
12 modulus does not depend on frequency. We can assume that, in this last regime, the  
13 oscillations are sufficiently large and fast to destroy all CSH, and that the time spent at rest

1 (zero shear rate) is too short to allow new CSH bonds to form. It thus allows us to isolate the  
2 colloidal interactions network. With this procedure, the measured answer of the system is  
3 therefore dominated by the elastic answer of the colloidal network. By applying such strain  
4 oscillations, it is then possible to study independently the kinetic of the colloidal network  
5 formation. Using this type of oscillation, we measure the evolution of the storage or elastic  
6 modulus with time as plotted in Fig. 8. 20 minutes after mixing, the same cement paste as  
7 above ( $W/C=0.4$ ) is pre-sheared at  $150s^{-1}$  for 200s. The oscillations are applied straight after  
8 the end of the pre-shear at a frequency of 10 Hz. It may be interesting to note that, in this  
9 regime, the storage modulus is lower than the viscous modulus and the system is only weakly  
10 elastic. The answer of the system at these high frequencies is indeed dominated by the viscous  
11 contribution of the sheared interstitial fluid. We focus now on the time needed to create this  
12 network. We can see in Fig. 8 that the elastic modulus increases during the first 10 s and then  
13 reaches a plateau. This means that, after 10s, the network is formed and does not evolve  
14 anymore. The colloidal percolation characteristic time is therefore of the order of a few  
15 seconds.

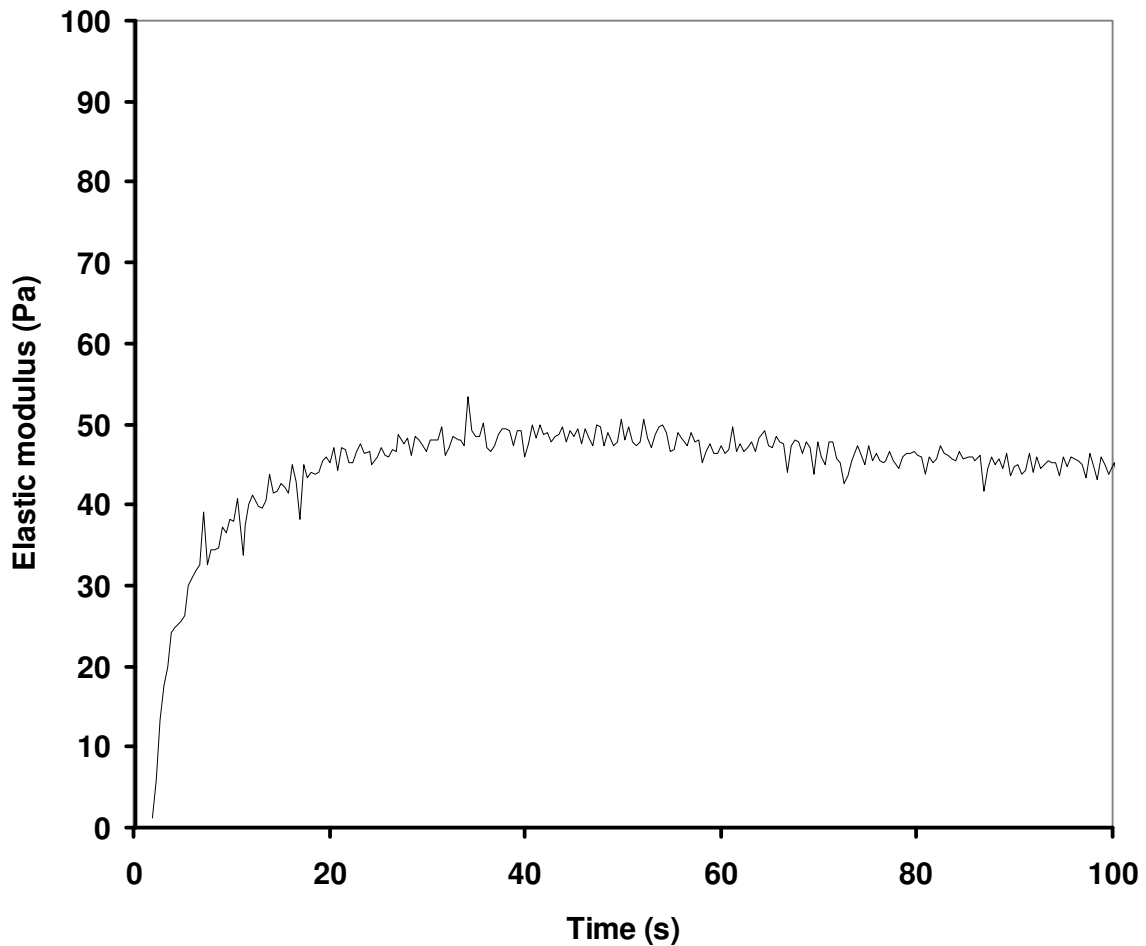
16

## 17 **3.2. Physical analysis**

### 18 **3.2.1. Colloidal percolation characteristic time**

19 In many colloidal suspensions in nature or industry, coagulation or flocculation are dictated  
20 by the competition between Brownian motion that tends to bring the particles into contact and  
21 viscous effects, that dissipate the particle kinetic energy and slow the coagulation or  
22 flocculation process down. It was however shown in [11] that, in the case of standard  
23 cementitious systems with particles average diameter  $d$  being of the order of  $10\mu m$ ,  
24 Brownian effects at short range are dominated by the attractive colloidal interactions  
25 described above. These attractive forces should replace, in the case of concentrated cement

1 suspensions, Brownian motion as the origin of the flocculation. The process shall be slowed  
2 down by the viscous dissipation associated with the drag force exerted on particles by the  
3 suspending fluid (*i.e.* water in most cases), the viscosity of which is noted here  $\mu_0$ .



4

5 *Figure 8. Storage modulus as a function of time for our W/C=0.35 cement paste. Frequency*  
6 *10Hz, amplitude 0.005.*

7

8 In the particular case of non retarded van der Waals interaction, which were shown to  
9 dominate the other colloidal interactions in the case of cement pastes and therefore dictate the  
10 inter-particle distance [31, 33],  $\Phi_0$  is the energy potential and can be written as [34] :

$$1 \quad \Phi_0 \cong \frac{A_0 a^*}{12H} \quad (1)$$

2 where  $a^*$  is the radius of curvature of the “contact” points,  $H$  is the surface to surface  
3 separation distance and  $A_0$  is the Hamaker constant.

4 Following the spirit of most coagulation theories [35-37] and assuming that cement grains can  
5 be described as mono-disperse particles, we introduce here the characteristic flocculation time

6  $T_{floculation}$  :

$$7 \quad T_{floculation} = \frac{3\mu_0}{4N\Phi_0} \quad (2)$$

8 with  $N$  the total number of cement particles per unit volume. We first assume that the order  
9 of magnitude of the inter-particle distance to be accounted in Eq. (2) is not the average inter-  
10 particle distance of the order of  $1\mu\text{m}$ . We expect that, in such a dense system, it should be  
11 very easy to create a percolation path. The first percolation path appearing in the system shall  
12 therefore only involve particles, which were already almost in contact before flow stops. We  
13 thus assume that the order of magnitude of the inter-particle distance to be considered in the  
14 computation of the energy potential  $\Phi_0$  is the surface to surface distance at the “pseudo”  
15 contacts points in the flocculated system.

16 Let us now try to evaluate the value of this characteristic flocculation time. The values of  $H$   
17 that may be found in literature are of the order of a few nm [26, 31, 38], consistently with the  
18 value of the rigid critical strain. The Hamaker constant value for  $\text{C}_3\text{S}$  is of the order of  $1.6 \cdot 10^{-20}$   
19 J [34]. The estimated value of  $a^*$  for cement particles is estimated to be of the order of a  
20 few hundreds nm [11]. We consider here that the volume fraction  $\phi$  of a standard cement  
21 paste is of the order of 40% with  $\phi = \left(1 + \rho_p W / \rho_w C\right)^{-1}$  where  $\rho_p$  and  $\rho_w$  are respectively the  
22 density of the cement grains and the density of water. The number of cement particles per unit  
23 volume may be roughly estimated as  $\phi d^{-3}$ . The Newtonian viscosity of water  $\mu_0$  is of the

1 order of  $10^{-3}$  Pa.s at room temperature. Using the above values, it is found that the  
2 characteristic flocculation time is of the order of a couple of seconds.

3 The above analysis and the results from Fig. 8 show that, for most cementitious systems,  
4 colloidal percolation (*i.e.* the situation in which the network formed by the flocculated  
5 particles is strong enough to resist stress) should occur in the first seconds following  
6 beginning of rest.

7

### 8 **3.2.2. From colloidal and rigid percolations to rigidification**

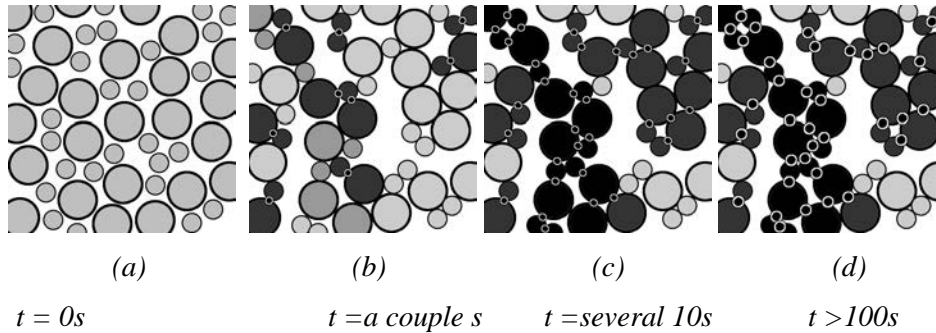
9

10 The result obtained in the previous section is not in agreement with [17] in which it was  
11 concluded that the time needed after the end of mixing to form a coagulated network of  
12 particles was of the order of a few minutes. It has however to be kept in mind that the strain  
13 oscillations amplitude in [17] was 0.03%. As described in section 3.1., this type of  
14 measurement is more representative of the consequences of the CSH nucleation than of the  
15 colloidal network evolution. It can therefore be concluded that the initial evolution in the  
16 material behavior measured during the first few minutes after the end of flow in [17] for very  
17 small strain amplitudes was not linked to colloidal flocculation and percolation but to CSH  
18 nucleation. It can moreover be concluded from the previous section that the initial evolution  
19 in the material behavior studied in [17] was in fact taking place in an already percolated  
20 colloidal network of cement particles.

21 We suggest here that there exists, after the colloidal network percolation, a transient phase,  
22 which finds its origin in the CSH nucleation. During this transient phase (that we will call  
23 here rigid percolation phase), the CSH nucleation turns locally the soft colloidal interaction  
24 between cement particles into a far more rigid interaction (*i.e.* higher energy potential), until a  
25 percolated network of cement particles with rigid interactions exist. In a second phase (that

1 we will call here rigidification phase), when all soft interactions have been turned into rigid  
 2 interactions, the continuing nucleation of CSH increases the rigidity by increasing either the  
 3 number of bridges between particles or by increasing the size of the bridges.

4



8 *Figure 9. Network(s) of interacting cement particles in the dormant period. All times are given as*  
 9 *orders of magnitude.*

10 (a) *Cement particles are dispersed at the end of the mixing phase ;*

11 (b) *A couple of seconds after the end of mixing, cement particles are flocculated forming a*  
 12 *percolated network of colloidal interactions. Darker particles belong to a percolation path ;*  
 13 *At the pseudo contact points between particles, nucleation of CSH (black and white dots) start*  
 14 *immediately to turn locally the soft colloidal interaction between cement particles into a far*  
 15 *more rigid interaction;*

16 (c) *All the particles in the percolation path (black particles) are linked by CSH bridges forming a*  
 17 *percolated rigid network in the material ;*

18 (d) *The elastic modulus of the mixture keeps on increasing as the size of the CSH bridges (black*  
 19 *and white dots) increase.*

20

21 Considering all the above, the following scheme can then be used to describe both short,  
 22 medium and long term evolutions of fresh cement pastes [24, 39] at rest during the dormant  
 23 period:

- 24 • At the end of mixing phase, cement particles are dispersed (Fig 9(a)).
- 25 • Because of colloidal attractive forces, cement particles flocculate in a few seconds and
- 26 form a network of interacting particles able to resist stress and displaying an elastic
- 27 modulus (Fig. 9(b)).



- 1 • Simultaneously, at the pseudo contact points between particles within the network,  
2 nucleation of CSH occurs although the material is still in the dormant period. This  
3 nucleation turns locally the soft colloidal interaction between cement particles into  
4 CSH bridges. As a consequence, at the macroscopic scale, the elastic modulus  
5 increases. After several tens of seconds (*e.g.* 100 s in [17], and 30 s here, see below), a  
6 percolation path of particles interacting purely through CSH bridges appears (Fig.  
7 9(c)).
- 8 • Further increase of the macroscopic elastic modulus comes from an increase of the  
9 size or numbers of CSH bridges between percolated cement particles (Fig. 9(d)).

10

### 11 **3.2.3. Kinetics of rigidification**

12

13 In order to go further in the analysis, we consider now a percolation path in the cement  
14 particles network (*i.e.* a succession of interacting cement particles able to transfer a  
15 macroscopic stress lower than the yield stress while keeping their respective positions). After  
16 the rigid percolation phase, this percolation path can be seen as a succession of cement  
17 particles interacting via rigid interactions due to CSH nucleation in the pseudo contact zones  
18 between these particles.

19 We assume that the bridges formed by the CSH between these cement grains can be  
20 considered as cylindrical homogeneous links of length  $H$  (the inter-particle distance) and of  
21 diameter  $D$  (see Fig. 10). We will consider in the following that both  $H$  and  $D$  are of the  
22 order of a couple nanometers whereas the diameter of the cement grains  $d$  is of the order of  
23  $10\mu\text{m}$ . The elastic modulus  $G'_{CSH}$  of the CSH forming the link can be found in literature and is  
24 of the order of a few tens of Gpa [41].

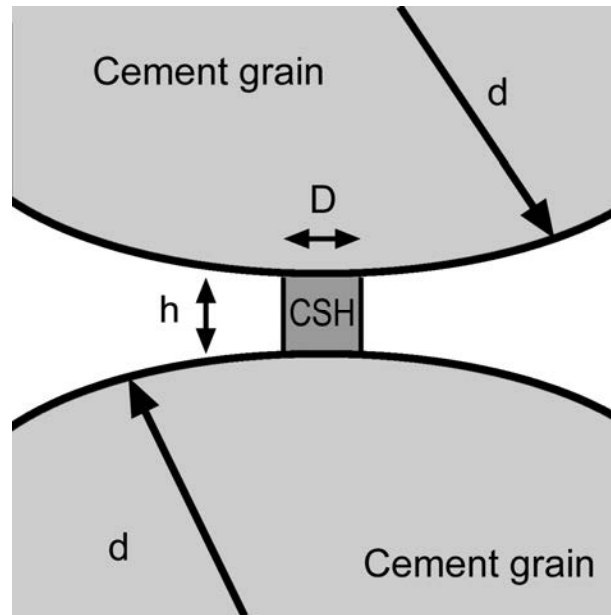


Figure 10. CSH bridge between two cement grains.

1  
2  
3  
4

5 From the simple geometry shown in Fig. 10, it is first possible to show that, when a  
6 macroscopic stress is applied to the system, because of geometry effects, the stress  
7 concentrates in the CSH bridge. As a first approximation, it is possible to write that the  
8 macroscopic stress  $\tau_{macro}$  applied to the percolated network and the local stress in the CSH  
9 bridge  $\tau_{CSH}$  are related by  $\tau_{macro} d^2 \approx \tau_{CSH} D^2$ . The stress in the CSH bridge is therefore  $10^8$   
10 times higher than the macroscopic stress.

11 Strain also concentrates in the CSH bridge. This local strain can be estimated as being  $d/H \approx$   
12  $10^4$  times higher than the macroscopic strain  $\gamma_{macro}$ . Therefore, when the rigid critical strain of  
13 order  $10^{-4}$  is applied to the system, the local CSH strain is of order 1. This can be considered  
14 as an unusually high value for the fracture strain of rigid mineral solids but it is a standard  
15 order of magnitude for a dense suspension of elongated colloidal particles such as CSH pellets  
16 [41].

1 Keeping in mind that  $\tau_{macro} = G'_{macro} \gamma_{macro}$  and  $\tau_{CSH} = G'_{CSH} \gamma_{CSH}$ , it is possible to write that  
 2  $G'_{macro} = G'_{CSH} D^2/dH$ . We then expect from this relation a macroscopic elastic modulus after  
 3 the rigid percolation phase  $10^4$  times lower than the elastic modulus of the CSH, *i.e.* of the  
 4 order of 1Mpa. This is not far from the values shown in Fig. 3 and Fig. 5 and close to the  
 5 values obtained in [17]. It can be noted that, in order to get more quantitative values of this  
 6 modulus, one would need to know the exact typology of the percolated network and use  
 7 micromechanical models taking into account the exact geometry of the percolated path under  
 8 consideration. This is however far beyond the scope of this paper.

9 Having checked the global consistency of our assumptions, we can now go further. We  
 10 assume that the ongoing CSH nucleation increases the cross section of the CSH bridges.  
 11 As the heat of hydration, after the initial peak, is constant in the so-called “dormant” phase, it  
 12 is possible to assume that the volume of hydrates at the contact points increases linearly with  
 13 time. As the inter-particle distance  $H$  is fixed (*i.e.* the cement particles network spatial  
 14 configuration stays unchanged [17]),  $D^2$  increases linearly with time and the macroscopic  
 15 elastic modulus of the cement paste (*i.e.* the strength of the cement particles network  
 16 interacting through CSH bridges)  $G'_{macro} = G'_{CSH} D^2/dH$  should also increase linearly with  
 17 time. This is the case in Fig. 5 after a few hundreds seconds. This would mean that, within the  
 18 above theoretical frame, the colloidal percolation phase ends a few seconds after the end of  
 19 the last strong shearing whereas the rigid percolation phase ends several hundreds of second  
 20 later. From that point, the rigidification phase starts, during which the elastic modulus  
 21 increases linearly with time.

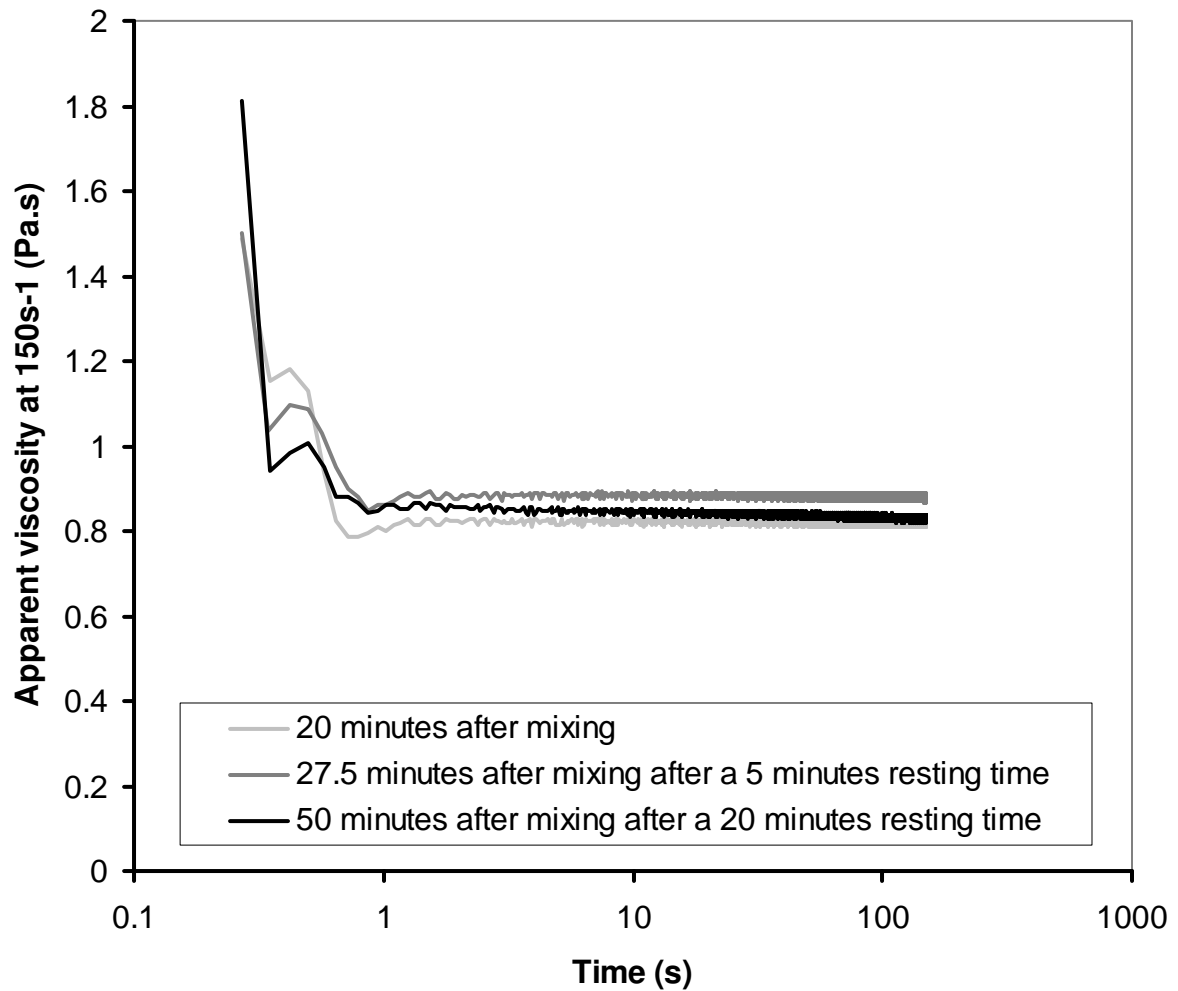
22

#### 23 **4. Thixotropy and apparent yield stress**

24

1 Thixotropy is a reversible macroscopic phenomenon and is therefore often associated to  
2 reversible physico-chemical phenomena such as flocculation and de-flocculation under shear  
3 of colloidal suspensions. It has however to be kept in mind that thixotropy is defined at a  
4 purely macroscopic level: it only implies that the macroscopic evolutions of the behavior of  
5 the material are reversible [3-9]. In the case of cement pastes, this means that, as long as shear  
6 is sufficient to bring the material back to a reference state, one does not have to care whether  
7 the evolution of the material behavior is due to colloidal flocculation or to CSH bridges  
8 between particles. Even if, at a microscopic scale, it is a non reversible chemical reaction that  
9 creates bonds between particles, these may be weak enough to be broken by shear whereas  
10 new bonds may spontaneously appear again at rest [24, 25] as long as the reservoir of  
11 chemical species is sufficient. Their formation is hence not incompatible with a macroscopic  
12 reversible evolution. From a practical point of view, hydration may therefore have reversible  
13 macroscopic consequences as long as the available mixing power is sufficient to break the  
14 CSH links between cement particles. Hydration is however at the origin of workability loss as  
15 soon as the available mixing power becomes insufficient to break these inter-particle  
16 connections [11, 24, 25], if we neglect here any chemical reactions between HRWRA and  
17 cement hydration [44].

18 We first check here that the thixotropic behavior of the  $W/C = 0.4$  cement paste tested in this  
19 paper is fully reversible at high shear rates. 20 minutes after mixing, we first shear the paste at  
20  $150 \text{ s}^{-1}$  for 150 s. We then leave it at rest for 5 minutes. In a third phase, we shear it again at  
21  $150 \text{ s}^{-1}$  for 150 s. We then leave it at rest for 20 minutes. In a final phase, we shear it once  
22 again at  $150 \text{ s}^{-1}$  for 150 s. We use once again the same rheometer and Vane tool. We compute  
23 the apparent viscosity using a Couette analogy [45], assuming that, at these high shear rates,  
24 the gap is fully sheared. We plot in Fig. 11 the apparent viscosity (*i.e.* the ratio between shear  
25 stress and shear rate) of the paste.



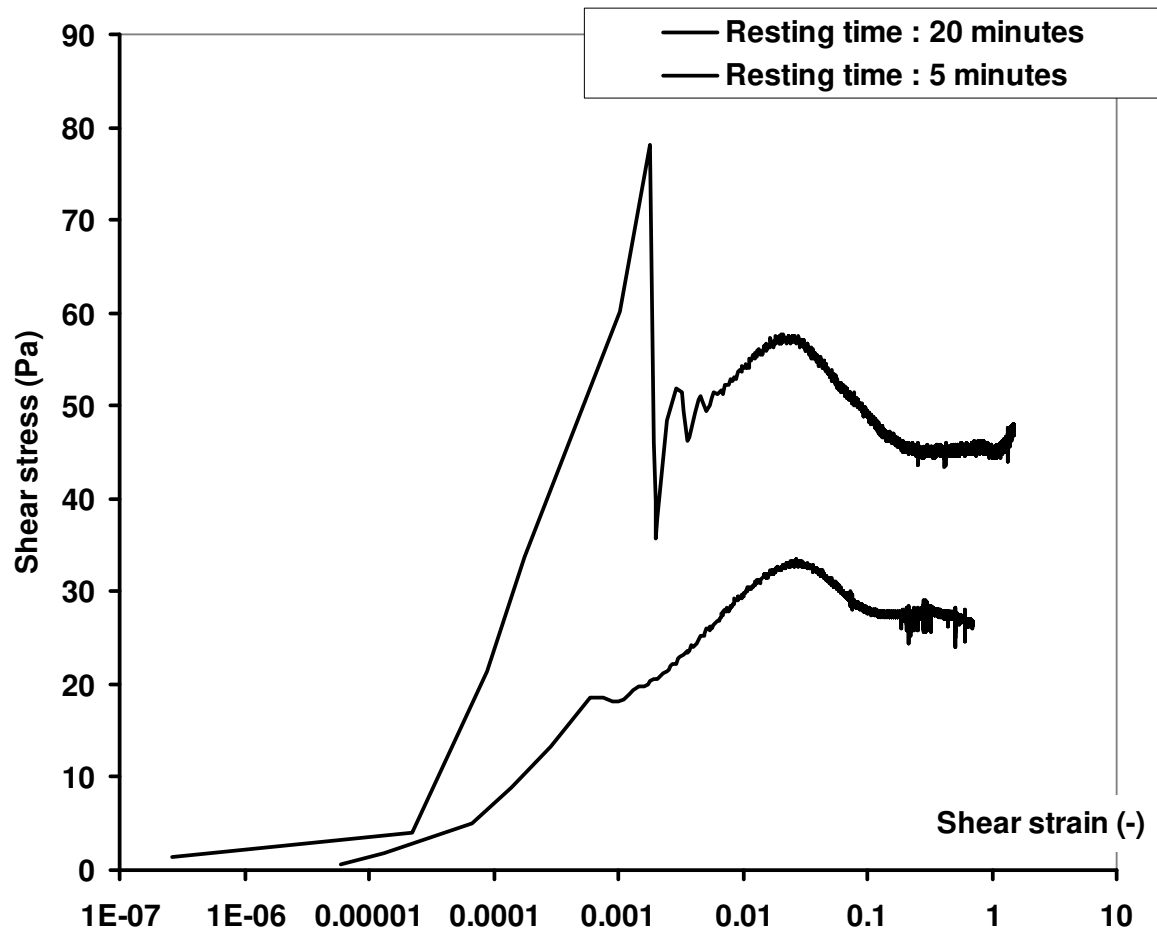
1

2 *Figure 11. Apparent viscosity as a function of time for our W/C=0.4 cement paste for*  
3 *successive shearings.*

4

5 In order to evidence the impact of hydration on the macroscopic reversible thixotropic  
6 behavior of a cement paste during the dormant period, we measure now the stress needed to  
7 initiate flow with our Vane tool after two resting times for our W/C = 0.4 cement paste at a  
8 shear rate of  $0.005\text{s}^{-1}$ . The results are plotted in Fig. 12.

9



1

2 *Figure 12. Shear stress as a function of strain during a Vane test for a water to cement ratio*  
 3 *of 0.4.*

4

5 We observe that, according to the resting time, the dominant peak stress will either be  
 6 associated to the rupture of a soft colloidal network (*i.e.* for a 5 minutes resting time, the  
 7 stress peak occurs at a strain of the order of a few %) or to the rupture of a rigid CSH based  
 8 network (*i.e.* at a longer resting time (20 minutes), the stress peak occurs at a strain of the  
 9 order of a few hundredths of %). The stress peak at a 0.0005 strain can be associated with the  
 10 rigid network only (the contribution of the soft colloidal network to stress at such strain being  
 11 negligible). It can also be seen that, although the soft critical strain does not change, the stress  
 12 peak associated to the rupture of the colloidal network is increasing with the time at rest. As  
 13 we have shown above in this paper that, after a few seconds, the colloidal network did not

1 evolve anymore (the elastic modulus being constant), it can therefore be concluded that the  
2 stress associated to this peak is the result of the combination of soft colloidal interactions and  
3 CSH bridges between particles formed at rest that were not all broken when the rigid critical  
4 strain was reached or that continuously broke and reformed all along the measurement.

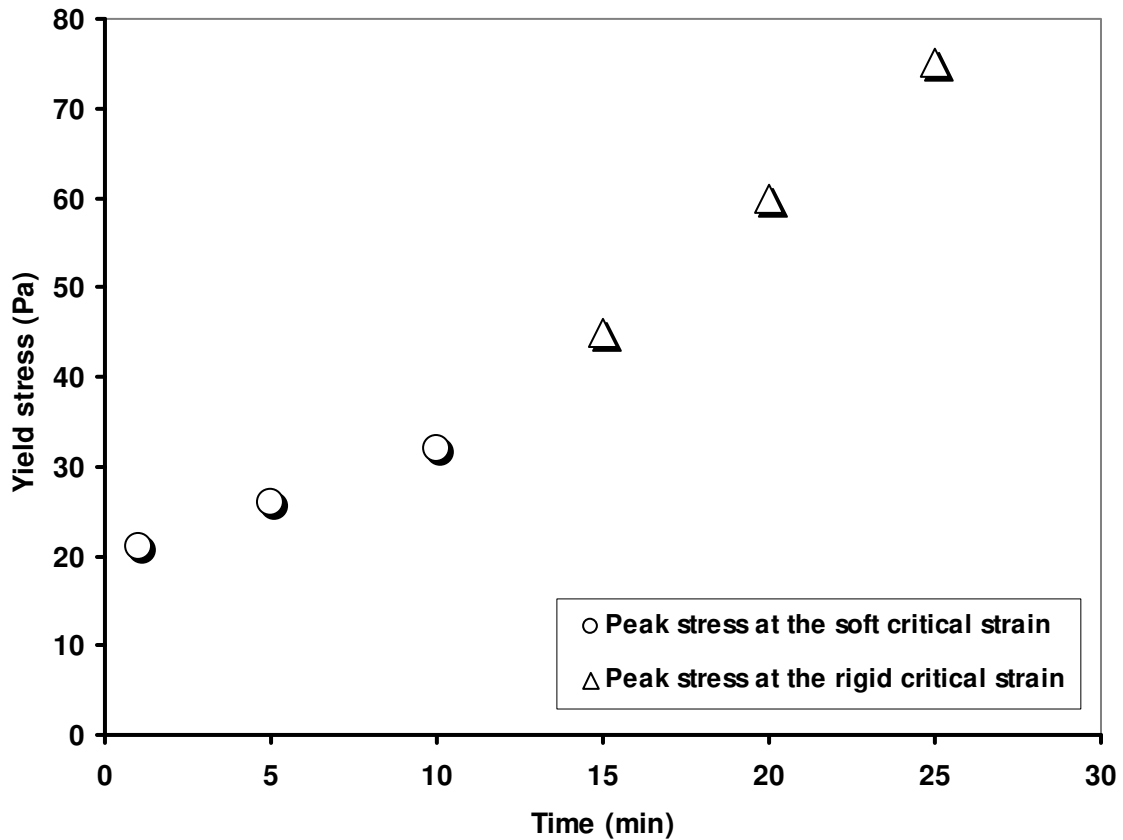
5 Other secondary comments can be made on Fig. 12. First, the strong fluctuations after the  
6 peak associated with the rupture of the rigid network at 20 minutes resting time are due to the  
7 rheometer, which is not able to keep on controlling accurately the strain rate during such an  
8 event. This illustrates the rigidity of this network, which breaks similarly to a fragile solid  
9 material.

10 Second, it can be seen in Fig. 12 that, contrary to Fig. 11, the material does not come back to  
11 the same reference state after the peak(s); this means that the yielding mechanism associated  
12 to the shear rate applied in this test (*i.e.*  $0.005\text{s}^{-1}$ ) does not bring the system to a fully  
13 dispersed state but probably leads to residual flocs of cement particles of higher average size  
14 than the individual cement particles [46], and whose precise size depends on how yielding has  
15 occurred.

16 It can be concluded from Fig. 12 that, according to the resting time, the measured apparent  
17 yield stress in practice will be the first or the second peak. As it was demonstrated that the  
18 critical strain associated to the rigid contact interactions does not change much with time [17]  
19 (*i.e.* it stays of the order of few hundredths of %) and we have shown above that the evolution  
20 of the rigid network elastic modulus associated to CSH nucleation is linear with time, the  
21 critical stress associated to the rupture of this network should also increase linearly with time.

22 As soon as this critical stress is the dominant one, the measured yield stress should also  
23 increase linearly with time. This explains why, in literature, most measurements of apparent  
24 yield stresses on observation periods of the order of 1 hour have shown linear evolution of the  
25 yield stress with time. This is also the case of the cement paste studied in this paper as shown

1 in Fig. 13. We plot in this figure the highest peak stress measured through the same Vane test  
2 as above for various resting times. For resting times lower than 10 minutes, this peak stress is  
3 measured for the soft critical strain. For larger resting times, it is measured for the rigid  
4 critical strain. In the particular case of the pastes tested in this paper, this limit corresponds to  
5 the end of the rigid percolation phase.



6

7 *Figure 13. Apparent or static yield stress as a function of resting time.*

8

9 It has finally to be kept in mind that what operators measure in most procedures and what  
10 matters in industrial practice is the value of the stress peak no matter its origin. Indeed,  
11 practical problems involving thixotropy include stability of coarse aggregates in cement paste,  
12 distinct-layers casting of SCC or formwork pressure prediction and are dictated by the  
13 evolution of the yield stress with time at rest at the scale of several tens of minutes [9].  
14 However, as we have shown above that colloidal flocculation only affects thixotropy on a few



1 seconds time scale and that even the evolution of the stress associated to the soft critical strain  
2 seems to be strongly affected by CSH nucleation, we suggest here that, in practice, thixotropy  
3 is mainly affected by CSH nucleation.

4 This explains why one of the most efficient ways to create very thixotropic concrete is to  
5 introduce hydration accelerating products in the mixture [47] or fine silica or limestone  
6 particles that will act as intercalated grains with strong nucleating properties. As soon as the  
7 mixing power available during industrial processes is sufficient to break the additional CSH  
8 bonds created by these products, they enhance thixotropy without any workability loss. The  
9 results obtained here also explain why temperature, which strongly affects the hydration  
10 chemical reaction, is also a strong thixotropy and sometimes workability loss enhancer [48].

11

## 12 **5. CONCLUSION**

13 We have first clarified in this paper the ambiguity in literature concerning the critical strain of  
14 fresh cement paste. Thanks to a detailed analysis of the macroscopic behavior of a paste, we  
15 have shown that there exist two critical strains. We attribute each of these critical strains to a  
16 specific physical and chemical phenomenon involved in the behavior of the paste in the fresh  
17 state.

18 The largest critical strain is of the order of a few % and can be associated to the network of  
19 colloidal interactions between cement particles. The time needed to form this network is of  
20 the order of a couple seconds.

21 The smallest critical strain is of the order of several hundredths of % and can be associated to  
22 the early hydrates, which form preferentially at the contact points between aggregated cement  
23 grains. It develops as soon as some particles are flocculated in the mixture. The development  
24 of the network of cement particles interacting via CSH bridges can be decomposed in two  
25 successive phases: a rigid percolation phase followed by a rigidification phase during which

1 the elastic modulus at low strain increases linearly in time. These have reversible macroscopic  
2 consequences as long as the available mixing power is sufficient to break the rigid links  
3 between cement particles. It is however at the origin of workability loss as soon as the  
4 available mixing power becomes insufficient to break these inter-particle connections.

5 The value of the apparent yield stress of the mixture left at rest results from the two above  
6 phenomena. Depending on resting time, the dominant stress peak observed during a static  
7 yield stress measurement will be either measured for the rigid critical strain (at long times) or  
8 for the colloidal critical strain (at short times). At the rigid critical strain, its value is only  
9 determined by the strength of the CSH bonds in the rigid network. At the colloidal critical  
10 strain, its value is also affected by CSH nucleation. As we have shown here that the evolution  
11 of the elastic modulus of the rigid network is, in most cases, linear with time, the long term  
12 structural build up of the material which is associated with the rigid network only, is also  
13 linear in time as often measured in literature.

14

## 15 **REFERENCES**

- 16 [1] Tattersall G.H., Banfill P.G.F., *The Rheology of Fresh Concrete*, Pitman, London, 1983.
- 17 [2] Roussel, N., *Rheology of fresh concrete: from measurements to predictions of casting*  
18 *processes*, *Materials and Structures*, Vol. 40(10), pp. 1001-1012, (2007).
- 19 [3] Barnes, H.A., "Thixotropy - a review", *J. Non-Newtonian Fluid Mech.*, vol. 70 (1997) pp.  
20 1-33.
- 21 [4] Lapasin, R., Longo, V., Rajgelj, S., *Thixotropic behaviour of cement pastes*, *Cement and*  
22 *Concrete Research*, vol. 9 (1979) pp. 309-318.
- 23 [5] Otsubo, Y., Miyai, S., Umeya, K., *Time-dependant flow of cement pastes*, *Cement and*  
24 *Concrete Research*, vol. 10 (1980) pp. 631-638.

- 1 [6] Banfill, P.F.G., Saunders, D.C., On the viscosimetric examination of cement pastes,  
2 Cement and Concrete Research, vol. 11 (1981) pp. 363-370.
- 3 [7] Papo, A., The thixotropic behaviour of white Portland cement pastes, Cement and  
4 Concrete Research, vol. 18 (1988) pp. 595-603.
- 5 [8] Roussel, N., Steady and transient flow behaviour of fresh cement pastes, Cement and  
6 Concrete Research, vol. 35(9) (2005) pp. 1656– 1664.
- 7 [9] Roussel, N., A thixotropy model for fresh fluid concretes: theory, validation and  
8 applications, Cement and Concrete Research, Vol. 36, pp. 1797-1806, (2006).
- 9 [10] Flatt, R.J., Towards a prediction of superplasticized concrete rheology, Materials and  
10 Structures, Vol. 27, pp. 289–300, (2004).
- 11 [11] Roussel, N., Lemaître, A., Flatt, R.J., Coussot, P., Steady state flow of cement  
12 suspensions: A micromechanical state of the art, Cement and Concrete Research, vol. 40, pp.  
13 77–84, (2010).
- 14 [12] Maloney, C.E., Lemaitre, A., Amorphous systems in athermal, quasistatic shear, Phys.  
15 Rev. E 74, 016118 (2006).
- 16 [13] Zukoski, C. F., Particles and suspensions in chemical engineering: Accomplishments and  
17 prospects, Chemical Engineering Science, Vol. 50(24), pp. 4073-4079, (1995).
- 18 [14] Hutzler, S., Weaire, D., Bolton, F., The effects of Plateau borders in the two-dimensional  
19 soap froth III. Further results, Philosophical Magazine Part B, Vol. 71(3), pp. 277-289, (1995)
- 20 [15] Mahaut, F., Mokeddem, S., Chateau, X., Roussel, N., Ovarlez, G., Effect of coarse  
21 particle volume fraction on the yield stress and thixotropy of cementitious materials, Cement  
22 and Concrete Research, vol. 38, pp. 1276–1285, 2008.

- 1 [16] Schmidt, G., Schlegel, E., Rheological Characterization of C-S-H phases-water  
2 suspensions, *Cement and Concrete Research*, Vol. 32, pp. 593-599, (2002).
- 3 [17] Nachbaur, L., Mutin, J.C., Nonat, A., Choplin, L., Dynamic mode rheology of cement  
4 and tricalcium silicate pastes from mixing to setting, *Cement and Concrete Research*, Vol. 31,  
5 pp. 183-192, (2001).
- 6 [18] Schultz, M.A., Struble, L., Use of oscillatory shear to study flow behavior of fresh  
7 cement paste, *Cement and Concrete Research*, Vol. 23, pp. 273-282, (1993).
- 8 [19] Billberg, P., (2003), Form pressure generated by self-compacting concrete, *Proceedings*  
9 *of the 3rd international RILEM Symposium on Self-Compacting Concrete, RILEM PRO33*  
10 *Reykjavik, Iceland*, pp. 271-280.
- 11 [20] Derec, C., Ducouret, G., Ajdari, A., Lequeux, F., Aging and nonlinear rheology in  
12 suspensions of polyethylene oxide-protected silica particles, *PHYSICAL REVIEW E* 67,  
13 061403 (2003).
- 14 [21] T. G. Mason, J. Bibette, and D. A. weitz, Yielding and Flow of Monodisperse Emulsions,  
15 *Journal Of Colloid And Interface Science* 179, 439-448 (1996)
- 16 [22] Ketz, R. J., R. K. Prud'homme, and W. W. Graessley, "Rheology of concentrated  
17 microgel solutions," *Rheol. Acta* 27, 531-539 (1988).
- 18 [23] Lei, W.G., Struble, L.J., Microstructure and flow behavior of fresh cement paste, *J. Am.*  
19 *Ceram. Soc.*, 80(8), (1997), pp. 2021-2028.
- 20 [24] Jiang, S.P., Mutin, J.C., Nonat, A., Studies on mechanisms and physico-chemical  
21 parameters at the origin of cement setting. 1. The fundamental processes involved during the  
22 cement setting, *Cement and Concrete Research*, vol. 25(4) (1995) pp. 779-789.

- 1 [25] Nonat, A, Mutin, J.C., Lecoq, X., Jiang, S.P., Physico-chemical parameters determining  
2 hydration and particle interactions during the setting of silicate cements, *Solid State Ionics*,  
3 vol. 101-103 (1997) pp. 923-930
- 4 [26] Flatt, R.J., Dispersion forces in cement suspensions, *Cement and Concrete Research*,  
5 Vol. 34, pp. 399–408, (2004).
- 6 [27] R.J.-M. Pellenq, J.M. Caillol, A. Delville, Electrostatic attraction between two charged  
7 surface: a (N,V,T) Monte Carlo simulation, *J. Phys. Chem., B* 101 (1997) 8584–8594.
- 8 [28] S. Lesko, E. Lesniewska, An. Nonat, J.-C. Mutin, J.-P. Goudonnet, Investigation by  
9 atomic force microscopy of forces at the origin of cement cohesion, *Ultramicroscopy* 86  
10 (2001) 11 –21.
- 11 [29] Flatt R.J., Bowen, P., Electrostatic repulsion between particles in cement suspensions:  
12 Domain of validity of linearized Poisson–Boltzmann equation for non-ideal electrolytes,  
13 *Cement and Concrete Research*, Vol. 33, pp. 781–791, (2003).
- 14 [30] Banfill, P.F.G, A discussion of the paper “Rheological properties of cement mixes” by  
15 M. Daimon and D.M. Roy, *Cement and Concrete Research*, Vol. 9, pp. 795-798, (1979).
- 16 [31] K. Yoshioka, E. Sakai, M. Daimon, A. Kitahar, Role of steric hindrance in the  
17 performance of superplasticizers in concrete, *J. Am. Ceram. Soc.*, Vol. 80(10), pp. 2667–  
18 2671, (1997).
- 19 [32] Zingg, A., Holzer, L., Kaech, A., Winnefeld, F., Pakusch, J., Becker, S., Gauckler, L.,  
20 The microstructure of dispersed and non-dispersed fresh cement pastes — New insight by  
21 cryo-microscopy, *Cement and Concrete Research*, Vol. 38, pp. 522–529, (2008).
- 22 [33] C.M. Neubauer, M. Yang, H.M. Jennings, Inter-particle potential and sedimentation  
23 behaviour of cement suspensions: effects of admixtures, *Advanced cement based materials*,  
24 Vol. 8, pp. 17– 27, (1998).

- 1 [34] Flatt, R.J., Bowen, P., Yodel: A Yield Stress Model for Suspensions, *J. Am Ceram Soc.*,  
2 Vol. 89 (4), pp. 1244-1256, (2006).
- 3 [35] Tomonori Fukasawa, Yasuhisa Adachi, Effect of floc structure on the rate of Brownian  
4 coagulation, *Journal of Colloid and Interface Science* 304 (2006) 115–118
- 5 [36] Tawari, L.S., Koch, D.L., Cohen, C., Electrical Double-Layer Effects on the Brownian  
6 Diffusivity and Aggregation Rate of Laponite Clay Particles, *Journal of Colloid and Interface*  
7 *Science* 240, 54–66 (2001)
- 8 [37] Baldwin, J.L., Dempsey, B.A., Effects of Brownian motion and structured water on  
9 aggregation of charged particles, *Colloids and Surfaces A: Physicochemical and Engineering*  
10 *Aspects* 177 (2001) 111–122.
- 11 [38] Kjeldsen, A.M., Flatt, R.J., Bergström, L., Relating the molecular structure of comb-type  
12 superplasticizers to the compression rheology of MgO suspensions, *Cement and Concrete*  
13 *Research*, Vol. 36, pp. 1231–1239, (2006).
- 14 [39] Platel, D. (2005), The impact of the polymer architecture on the physico-chemistry  
15 properties of cement slurries. PhD thesis, ESPCI, Paris.
- 16 [40] S. Garrault, L. Nicoleau, A. Nonat, Tricalcium silicate hydration modeling and numerical  
17 simulations, *Proceeding of CONMOD 2010*, Lausanne, July 2010.
- 18 [41] M. Van Damme, The Nanogranular Origin of Concrete Creep: A Nanoindentation  
19 Investigation of Microstructure and Fundamental Properties of Calcium-Silicate-Hydrates,  
20 Thesis, MIT, Cambridge.
- 21 [42] M. Zajak, S. Garrault, J.P. Korb, A. Nonat, Effect of temperature on the development of  
22 C-S-H during early hydration of C3S, *Proceedings of 12th International Congress on the*  
23 *Chemistry of Cement*, Montréal, Canada, July 8 -13, 2007.

- 1 [43] S. Garrault, H. Minard, A. Nonat, Hydration of silicate phase and mechanical evolution in  
2 “alite-tricalcium aluminate-gypsum” complex system, Proceedings of 12th International  
3 Congress on the Chemistry of Cement, Montréal, Canada, July 8 -13, 2007.
- 4 [44] Flatt, R.J., Houst, Y.F., A simplified view on chemical effects perturbing the action of  
5 superplasticizers, *Cement and Concrete Research*, vol. 31 (2001) pp. 1169–1176.
- 6 [45] Estellé, P., Lanos C, Perrot, A., Amziane, S. (2008), Processing the vane shear flow data  
7 from Couette analogy, *Appl Rheol*, 18, 34037-34481.
- 8 [46] Masschaele, K., Fransaer, J., Vermant, J., Direct visualization of yielding in model two-  
9 dimensional colloidal gels subjected to shear flow, *J. Rheol.* Vol. 53(6) (2009) pp. 1437-1460.
- 10 [47] Roussel, N., Cussigh, F., Distinct-layer casting of SCC: the mechanical consequences of  
11 thixotropy, *Cement and Concrete Research*, vol. 38, (2008), pp. 624-632.
- 12 [48] Petit, J.Y., Khayat, K.H., Wirquin, E., Coupled effect of time and temperature on  
13 variations of yield value of highly flowable mortar, *Cement and Concrete Research*, Vol. 36,  
14 pp. 832–841, (2006).

15